JOURNAL OF AIRCRAFT
Vol. 34, No. 4, July–August 1997

# Engineering Notes

*ENGINEERING NOTES are short manuscripts describing new developments or important results of a preliminary nature. These Notes cannot exceed 6 manuscript pages and 3 figures; a page of text may be substituted for a figure and vice versa. After informal review by the editors, they may be published within a few months of the date of receipt. Style requirements are the same as for regular contributions (see inside back cover).*

## Enhanced Aerofoil Performance Using Small Trailing-Edge Flaps

A. W. Bloy,* N. Tsioumanis,† and N. T. Mellor‡
*University of Manchester,*
*Manchester M13 9PL, England, United Kingdom*

### Introduction

IMPROVED aerofoil performance using a small trailing-edge flap was first reported by Liebeck,[1] in tests made on a Newman symmetric aerofoil with a Gurney flap. This type of flap is positioned at the trailing edge on the lower surface and is perpendicular to the surface. In Liebeck's tests,[1] a Gurney flap depth of 1.25% of the wing chord was used, increasing the lift and lift-to-drag ratio for lift coefficients greater than 1. The application of this device to a racing car wing improved both its maximum speed and down force in cornering.

To explain the reduced drag at high angle of attack, Liebeck[1] presented a model of the flowfield in the region of the Gurney flap, which has been substantiated by flow visualization tests made in a water tunnel by Neuhart and Pendergraft.[2] In the water tunnel, the Gurney flap provided an increased region of attached flow on the wing upper surface with a recirculation region behind the flap. This is consistent with the reduced form drag obtained at high lift coefficient using a Gurney flap.

Other works have confirmed this finding.[3–6] However, Bloy and Durrant[3] found that the performance of an aerofoil with a small 45-deg trailing-edge flap is superior to the same wing with a similarly sized Gurney flap. Both types of flaps significantly increase the maximum lift of the NACA $63_2$-215 aerofoil, although the 45-deg flap produces less drag than the Gurney flap. Of the flaps tested, a 2% chord 45-deg flap produced the highest lift, with the lift-to-drag ratio higher than that of the aerofoil with the Gurney flap over the entire angle-of-attack range. The peak lift-to-drag ratio with the 45-deg flap is comparable to that of the wing without flap, but at a higher lift coefficient.

Although the Gurney and 45-deg flaps give enhanced performance at high lift, there is a drag penalty at low lift, particularly in the case of the Gurney flap. Part of the drag increment is probably because of the forward-facing step on both flaps.

The purpose of the present study was to test and compare five flap shapes with the same flap length. Figure 1 defines the dimensions of the 90-deg Gurney flap, the 90-deg wedge flap, the square section flap, the 45-deg flap, and the 45-deg wedge flap. The wedge flaps and square section flap have the advantage of being more rigid than the 45- or 90-deg flaps, making them easier to apply to the wing. A similar wedge flap formed by filling in the pressure side of a Gurney flap has been tested.[2,7]

### Experimental Setup

An untwisted, rectangular wing of 0.152 m chord and 0.762 m span was used in the tests performed in a low-speed wind tunnel, with a 0.87 × 1.13 m closed test section. The aerofoil section used is the NACA 5414 section. Force and moment measurements were taken using a six-component balance with appropriate wind-tunnel strut, wall interference, and flow misalignment corrections made. The tunnel airspeed for all of the tests was 52 m/s, giving a Reynolds number based on the wing chord of $0.57 \times 10^6$. The turbulence intensity in the test section is 0.6%. Measurements were first made using the plain wing, and then with the five full-span trailing-edge flaps attached to the wing using double-sided adhesive tape.

The wind-tunnel data acquisition system provided excellent repeatability, as 500 samples were taken at each point. The errors in the measured lift, drag, and pitching moment coefficients are less than 1%.

### Experimental Results

The variation of the lift coefficient $C_L$ and drag coefficient $C_D$, with angle of attack $\alpha$, are shown in Figs. 2 and 3. Compared with the plain wing, all flaps, with the exception of the 45-deg wedge flap, produce similar lift increment and maximum lift coefficient with the 45-deg wedge flap, producing slightly less lift. However, the lowest drag increment throughout the incidence range is produced by the 45-deg wedge flap with the 90-deg Gurney flap, producing a significant drag penalty at low to moderate angle of attack. At high angle of attack, the difference between the wing drag with all five flaps is proportionally less.

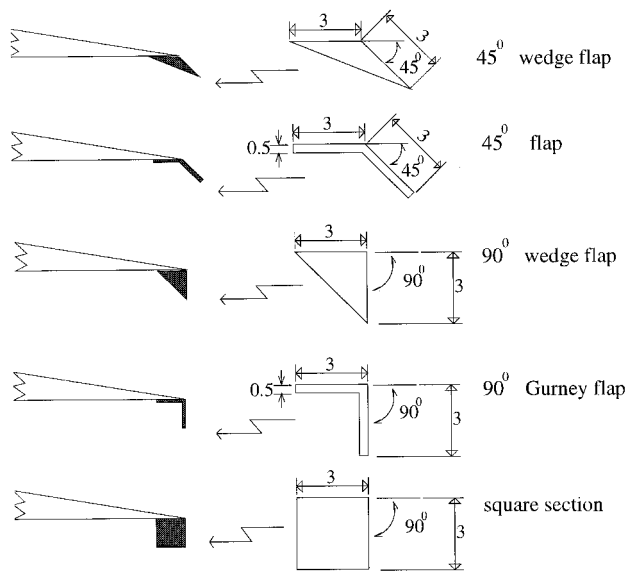


**Fig. 1 Dimensions of trailing-edge flaps (all dimensions in millimeters).**

Received Jan. 15, 1997; revision received April 4, 1997; accepted for publication April 8, 1997. 

*Lecturer, Aerospace Engineering Division, School of Engineering.
†Research Student, Aerospace Engineering Division, School of Engineering.
‡Student, Aerospace Engineering, School of Engineering.

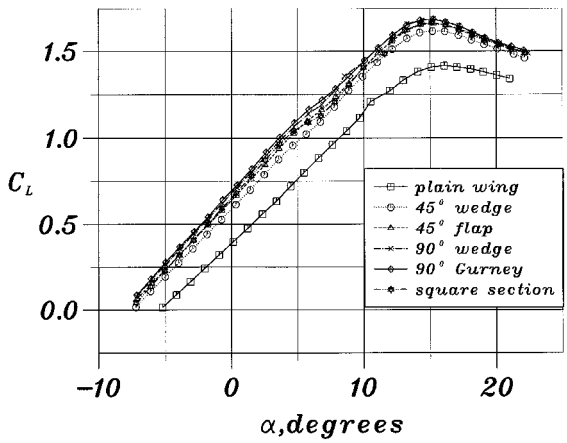


**Fig. 2 Variation of lift coefficient with angle of attack.**

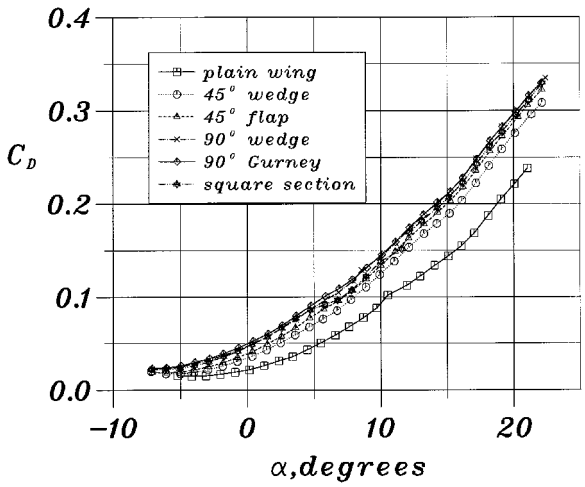


**Fig. 3 Variation of drag coefficient with angle of attack.**

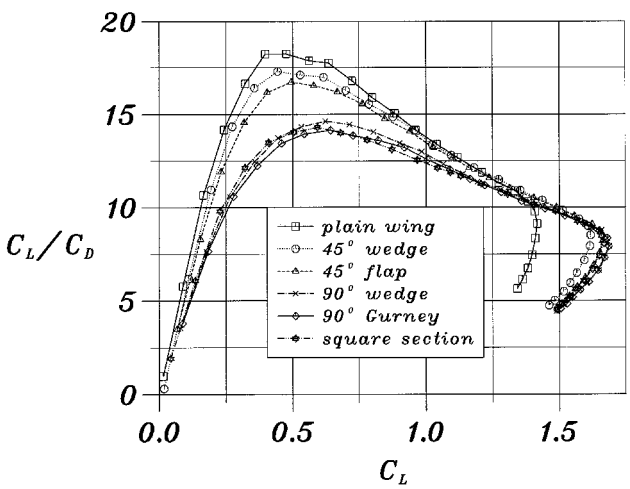


**Fig. 4 Variation of lift-to-drag ratio with lift coefficient.**

Figure 4, which shows the effects of the five flaps on the lift-to-drag ratio, is in agreement with previous results.[3–7] Enhanced lift capability is accompanied by a reduction in the lift-to-drag ratio at low to moderate lift. This is clearly observed for the 90-deg Gurney flap and square section flap, which have the lowest lift-to-drag ratio. Some improvement is achieved by the 90-deg wedge flap, although the performance is still inferior to that of the 45-deg flap. Further improvement in the performance is obtained from the 45-deg wedge flap, which has a maximum lift-to-drag slightly less than that of the plain wing. However, this is achieved with a slight reduction in the maximum lift compared with the other flaps.

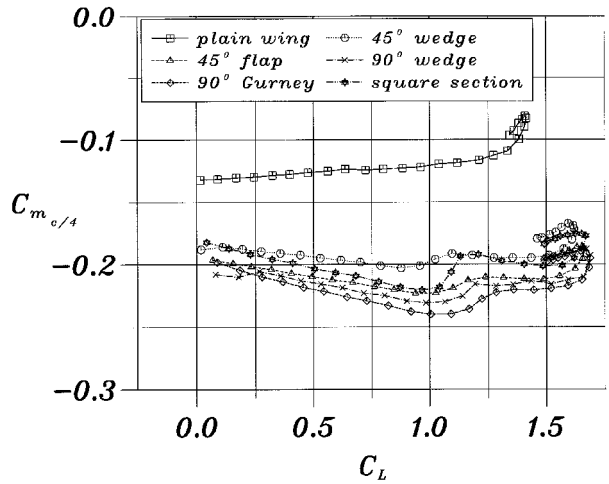


**Fig. 5 Variation of pitching moment coefficient about quarter-chord line with lift coefficient.**

Finally, the nose-down pitching moment about the quarter-chord line $C_{m_{c/4}}$ is shown in Fig. 5. The pitching moment increment appears to be proportional to the lift coefficient increment caused by the flaps.

Note that a small part of the measured force and moment increments produced by the 45-deg flaps is in proportion to the increase in the chord length. This effect enhances the lift, drag, and pitching moment coefficients, which are based on the chord of the plain wing, by the relatively small amount of 1.4%. It might, therefore, be expected that the lift-to-drag ratio is unaffected, but the increase in chord length leads to a reduction in the wing aspect ratio and an increase in induced drag. The overall effect is to slightly reduce the lift-to-drag ratio for the 45-deg flaps.

## Conclusions

All five flaps tested, the 2% chord 90-deg Gurney, 90-deg wedge, square section, 45-deg flap, and 45-deg wedge flaps, enhanced the maximum lift to a similar extent with the exception of the 45-deg wedge flap that produced slightly less lift. A relatively small part of the lift increase, in the case of the 45-deg flaps, is caused by the 1.4% increase in the chord length. In all cases there is a drag penalty at low to moderate lift. The 45-deg flaps give superior lift-to-drag over the angle-of-attack range compared with the 90-deg flaps. For both the 45- and 90-deg flaps, the lift-to-drag is enhanced by the addition of the upstream facing wedge with the 45-deg wedge flap giving a maximum lift-to-drag slightly less than that of the plain wing.

## References

[1]Liebeck, R. H., "Design of Airfoils for High Lift," AIAA Paper 80-3034, March 1980.

[2]Neuhart, D. H., and Pendergraft, O. C., "A Water Tunnel Study of Gurney Flaps," NASA TM 4071, Nov. 1988.

[3]Bloy, A. W., and Durrant, M. T., "Aerodynamic Characteristics of an Aerofoil with Small Trailing Edge Flaps," *Wind Engineering*, Vol. 19, No. 3, 1995, pp. 167–172.

[4]Kentfield, J. A. C., "The Potential of the Gurney Flap for Improving the Performance of Wind-Turbine Blading," *Proceedings of the Windpower '91*, American Wind Energy Association, Washington, DC, 1991, pp. 475–481.

[5]Roesch, P., and Vuillet, A., "New Designs for Improved Aerodynamic Stability on Recent Aerospatiale Helicopters," *Vertica*, Vol. 6, No. 3, 1982, pp. 145–164.

[6]Storms, B. L., and Jang, C. S., "Lift Enhancement of an Airfoil Using a Gurney Flap and Vortex Generators," *Journal of Aircraft*, Vol. 31, No. 3, 1994, pp. 542–547.

[7]Kentfield, J. A. C., "The Influence of Free-Stream Turbulence Intensity on the Performance of Gurney-Flap Equipped Wind-Turbine Blades," *Wind Engineering*, Vol. 20, No. 2, 1996, pp. 93–106.

# Exact Leading-Term Solution for Low Aspect Ratio Wings

S. C. Rajan* and S. Shashidhar†
*Indian Institute of Technology, Madras 600036, India*

## Introduction

An exact solution is available for the ideal two-dimensional flow past a flat plate at low angles of attack for which the aspect ratio is infinity. The exact solution is easily worked out for the other extreme case of aspect ratio being zero. In this case the flat plate wing has a finite span and is semi-infinitely long, i.e., has a leading edge, but the trailing edge is at infinity. For this case it comes out naturally that the circulation distribution is elliptic and is independent of the shape of leading edge. In the present work the momentum theorem is used to obtain the expression for the leading-edge suction force as it brings out some subtle features that are not seen when the conservation of energy is applied. Sears[1] also makes use of the momentum theorem for calculating induced drag for a high aspect ratio elliptic wing.

## Wing in Translation

### Basic Theory and Calculation of the Normal Load

In Fig. 1 a semi-infinitely long flat plate having span length $2b$ and chord length infinity is shown exposed to a uniform stream $V_\infty$ at an angle of attack $\alpha$. The flat plate can be replaced by a vortex sheet and at the Trefftz plane, since the flow becomes two dimensional, the flowfield is known.

From the two-dimensional theory it is known that

$$\gamma_x(\infty, y) = 2V_\infty y \sin\alpha/\sqrt{b^2 - y^2} \tag{1}$$

where $\gamma_x$ is the intensity of vorticity at the Trefftz plane. It can be readily verified that it satisfies the no-penetration boundary condition. Far downstream the value of $\gamma_y = 0$, and at the leading edge $\gamma_x = 0$. Hence, as we start at infinity at the port side of the wing and move toward the leading edge, the vortex lines gradually start curving, eventually intersecting the midspan line, turn, and on reaching infinity at the starboard side, become straight (Fig. 1). At any point on the vortex sheet

$$\boldsymbol{\gamma} = \gamma_x \boldsymbol{i} + \gamma_y \boldsymbol{j}$$

Using Bernoulli's equation it is easily shown that the pressure change $\Delta p$ across the plate is

$$\Delta p = \rho\gamma_y V_\infty \cos\alpha$$

Hence, the total normal load $F_z$ is

$$F_z = \rho V_\infty \cos\alpha \int_{-b}^{b} dy \int_0^\infty \gamma_y \, dx \tag{2}$$

**Fig. 1 Flat plate and its corresponding vortex system.**

The circulation $\Gamma$ at a span location $y$ is

$$\Gamma = \int_0^\infty \gamma_y \, dx \tag{3}$$

From Helmholtz's conservation equation it follows that

$$\gamma_x(\infty, y) = -\frac{d\Gamma}{dy} \tag{4}$$

Substituting for $\gamma_x$ from Eq. (1) and integrating Eq. (4) results in

$$\Gamma = 2V_\infty \sin\alpha\sqrt{b^2 - y^2} \tag{5}$$

It is seen that the expression for $\Gamma$ is elliptic. Combining Eqs. (2), (3), and (5) the normal load is obtained as

$$F_z = \pi\rho V_\infty^2 b^2 \sin\alpha \cos\alpha$$

### Calculation of the Inplane Suction Force

This is easily worked out considering a cylindrical control volume such that its axis is coincident with the $x$ axis. It has a radius $R$ and its upstream and downstream bounding planes are at distances $k_1R$ and $k_2R$ from the origin, where $k_1$ and $k_2$ are positive constants and could be equal. In the following analysis, surfaces 1 and 2 refer to the upstream and the downstream bounding planes, respectively, and 3 refers to the curved cylindrical surface. For estimating the order of magnitude of the velocity and the remaining quantities on the bounding surfaces, the wing is replaced by a single horseshoe vortex.

From the momentum theorem it is known that

$$F_x = -\int_{1+2+3} P \, dS - \int_{1+2+3} \rho V_n u \, dS \tag{6}$$

The contribution of 3 to the momentum integral, which is caused by the combined effect of the trailing vortices and the bound vortex, is first evaluated. Let $(x, y, z)$ be any point on surface 3. The normal velocity $V_n$ to the surface 3 satisfies $V_n(x, y, -z) = -V_n(x, y, +z)$. Also, $u = V_\infty \cos\alpha + u'$, where $u'$ is only caused by the bound vortex and satisfies the relation $u'(x, y, -z) = -u'(x, y, +z)$. Hence, $\int_3 \rho V_n u \, dS$ reduces to $\int_3 \rho V_n u' \, dS$. Now, $V_n = \mathbb{O}(1/R^2)$, $u' = \mathbb{O}(1/R^2)$ and the area of surface 3 is of the $\mathbb{O}(R^2)$ and, therefore, $\int_3 \rho V_n u' \, dS \to 0$ as $R \to \infty$.

Similarly, the combined contribution of planes 1 and 2 to the momentum integral is zero. Hence, there is only the pressure integral contribution to the suction force and Eq. (6) reduces to

$$F_x = -\int (P_{d\infty} - P_{u\infty}) \, dS \tag{7}$$

where $P_{d\infty}$ and $P_{u\infty}$ represent the pressures far downstream and far upstream, respectively. From Bernoulli's equation it follows that

$$P_{d\infty} - P_{u\infty} = -\tfrac{1}{2}\rho[(v'^2 + w'^2) + 2V_\infty \sin\alpha \, w']$$

Received Nov. 25, 1996; revision received Jan. 20, 1997; accepted for publication March 3, 1997. 

*Assistant Professor, Department of Aerospace Engineering.
†Research Scholar, Department of Aerospace Engineering.